

Spectroscopic metallicities of Vega-like stars

C. Saffe^{1,*}, M. Gómez², O. Pintado³, and E. González⁴

¹ Complejo Astronómico El Leoncito, CC 467, 5400 San Juan, Argentina

e-mail: csaffe@casleo.gov.ar

² Observatorio Astronómico de Córdoba, Laprida 854, 5000 Córdoba, Argentina

e-mail: mercedes@oac.uncor.edu

³ Instituto Superior de Correlación Geológica (INSUGEO), 4000 Tucumán, Argentina

e-mail: opintado@tucbbs.com.ar

⁴ Facultad de Ciencias Exactas, Físicas y Naturales (UNSJ), 5400 San Juan, Argentina

e-mail: erip.p.a.gonzalez@gmail.com

Received September 15, 1996; accepted March 16, 1997

ABSTRACT

Aims. To determine the metallicities of 113 Southern Hemisphere Vega-like candidate stars in relation to the Exoplanet host group and field stars.

Methods. We applied two spectroscopic methods of abundance determinations: equivalent width measurements together with the ATLAS9 (Kurucz 1993) model atmospheres and the WIDTH9 program, and a comparison of observed spectra with the grid of synthetic spectra of Munari et al. (2005).

Results. For the Vega-like group, the metallicities are indistinguishable from those of field stars not known to be associated with planets or disks. This result is quite different from the metallicities of Exoplanet host stars which are metal-rich in comparison to field stars.

Key words. Techniques: spectroscopic – Stars: abundances – Stars: late-type

1. Introduction

It is well established that Exoplanet host stars are, on average, metal-rich in comparison to stars that do not harbor Doppler detected planets (see, for example, Santos et al. 2004). Two hypotheses have been put forward to explain this peculiarity of the Exoplanet host stars a) a primordial origin and b) a pollution of the convective zone of the star. In the first case the "excess" of metallicity was already present in the parent cloud from which the star bearing planet/s was formed (see, for example, Santos et al. 2001). In the pollution scenario the convective zone of the star is contaminated by the infall or accretion of planets and/or planetesimals (see, for example, González et al. 2001).

Santos et al. (2004) found a lack of correlation between the thickness of the convective zone and the metallicity for a sample of FG dwarfs with planets. As the convective zone acts as a diluting medium, for a given amount of accreted material, F dwarfs with thinner convective zones should exhibit a greater degree of pollution than G dwarfs with thicker zones. On average, F and G dwarfs

* On a fellowship from CONICET, Argentina.

exhibit similar metallicities and the pollution hypothesis is not favored by these observations. The primordial origin of the "excess" remains an alternative to explain the relatively high metallicity of stars with planets with respect to field stars.

However, Pasquini et al. (2007) compared the metallicities of giant and dwarf stars with planets and found that the first group has, on average, lower metallicities than the dwarfs. The smaller mass of the convective zone of the dwarfs with respect to the giants provides a plausible explanation for this difference. The diluting effect of the convective zone is efficient for the giants and tends to lower the metallicity to its primordial value. In this case, the pollution scenario is favored (over the primordial origin) since it can explain the observed difference in metallicities between dwarfs and giants with planets. Even when the origin or the cause of the "excess" of metallicity of stars with planets is not well understood, the Exoplanet host stars are metal-rich and this is a feature that distinguishes this group among stars with similar physical properties and no giant planets detected.

Vega-like stars are a group of objects that show infrared excesses in their spectral energy distributions that can be attributed to the presence of dust in circumstellar disks. The first members or candidate members of the class were selected by IRAS and had mainly A-F spectral types (Aumann et al. 1984; Gillett 1986; Backman & Paresce 1993; Sylvester et al. 1996; Mannings & Barlow 1998; Fajardo-Acosta et al. 1999; Sylvester & Mannings 2000; Habing et al. 2001; Laureijs et al. 2002; Sheret et al. 2004). Vega (α Lyr) is one of the four prototypes of the group or the "fabulous four" (Vega, β Pictoris, Fomalhaut = α PsA and ϵ Eridanis; Gillett 1986) and has given the name to the class.

More recently, Spitzer has contributed with the detection of G dwarfs with infrared excesses (Meyer et al. 2004; Rieke et al. 2005; Kim et al. 2005; Chen et al. 2005; Uzpen et al. 2005; Beichman et al. 2005, 2006; Bryden et al. 2006; Silverstone et al. 2006; Su et al. 2006; Trilling et al. 2008). Since the excesses come from distances similar to the Kuiper-Belt to the Sun, these stars have also received the designation of Kuiper-Belt analogs or Kuiper-Belt-like stars. In this contribution we adopt the term "Vega-like stars" to refer to both IRAS and Spitzer detections.

The metallicity of Vega-like stars has previously been investigated by Greaves et al. (2006) and Chavero et al. (2006), deriving nearly solar values. However these works analyzed relatively small samples of objects. Greaves et al. (2006) studied a group of 18 FGK Vega-like stars whereas Chavero et al. (2006) included 42 FG dwarfs with infrared excesses in their metallicity determination. In addition these previous works do not include stars of A spectral type which represent the bulge of IRAS detections. Greaves et al. (2006) derived their sample from the Doppler searches for planets that in general include solar type stars. Chavero et al. (2006) used the Strömberg photometry to determine the metallicity. These authors were also restricted to late spectral types.

Both the stars with planets and the Vega-like stars have evidence of the presence of circumstellar material, in the form of planet/s, in the first case, or dust in a circumstellar disk, in the second. As mentioned before, the Exoplanet hosts are metal-rich. This fact may have facilitated the formation of planets (Pollack et al. 1996). In this contribution we determine spectroscopic metallicities of a large sample of Vega-like stars to compare with the Exoplanet host group. We include objects of B–K spectral types, observable from the Southern Hemisphere.

2. The sample

We compiled a total of 113 Southern Hemisphere Vega-like candidate stars from the literature, based on their infrared or submillimetric excess emissions (Backman & Paresce 1993; Sylvester et al. 1996; Mannings & Barlow 1998; Fajardo-Acosta et al. 1999; Sylvester & Mannings 2000; Habing et al. 2001; Laureijs et al. 2002; Sheret et al. 2004). This compilation also includes G dwarfs with infrared excess recently detected by Spitzer (Beichman et al. 2005, 2006; Bryden et al. 2006; Su et al. 2006; Trilling et al. 2008). Specifically the list comprises objects with BAFGK spectral types (22, 38, 28, 17 and 8, respectively). All the stars are luminosity class V (Hipparcos catalogue) and have distances between 5 and 300 pc. Table 1 lists the observed objects.

Table 1 includes a sub-sample of stars that were originally selected by IRAS as candidate Vega-like stars. However, when observed by Spitzer the infrared excesses were deemed to be of little significance. These objects are: HD 10800, HD 20794, HD 38393, HD 41700, HD 68456, HD 160691, HD 169830, HD 203608, and HD 216437 (Beichman et al. 2005, 2006; Bryden et al. 2006; Hillenbrand et al. 2008; Trilling et al. 2008). For example, Bryden et al. (2006) found that for HD 10800 $\frac{f_{\text{MIPS-70}\mu\text{m}}}{f_s} = 1.3$ (the observed flux over the photospheric emission at 70 μm) and $\frac{f_{\text{MIPS-70}\mu\text{m}}}{f_s} = 1.2$ for HD 68456. This group of objects should be considered with caution.

3. Observations and data reduction

The stellar spectra were obtained at the Complejo Astronomico El Leoncito (CASLEO), using the *Jorge Sahade* 2.15-m telescope equipped with a REOSC echelle spectrograph¹ and a TEK 1024×1024 CCD detector. The REOSC spectrograph uses gratings as cross dispensers. We used a grating with 400 lines mm^{-1} , covering the spectral range $\lambda\lambda 3500\text{--}6500$, giving a resolving power of ~ 12500 . Three individual spectra for each object were obtained in four observing runs: August 05–08 2005, August 18–22 2005, February 18–25 2006 and May 04–07 2007 and have S/N ratio of about 300.

The spectra were reduced using IRAF² standard procedures for echelle spectra. We applied bias and flat corrections and then normalized order by order with the *continuum* task, using 7–9 order Chebyshev polynomials. We also corrected by the scattered light in the spectrograph (*apscatter* task). We fitted the background with a linear function on both sides of the echelle apertures, using the task *apall*. The resolution of the reduced spectra is 0.17 $\text{\AA}/\text{pix}$.

4. Metallicity determinations

We used two different methods of abundance determination: 1) Fe lines equivalent width measurements together with the ATLAS9 (Kurucz 1993) model atmosphere corresponding to a given star and the WIDTH9³ program. 2) A comparison of the observed and synthetic spectra using the Downhill method (Gray et al. 2001). In particular we used the grid of synthetic spectra calculated

¹ On loan from the Institute d’Astrophysique de Liege, Belgium.

² IRAF is distributed by the National Optical Astronomical Observatories which is operated by the Association of Universities for Research in Astronomy, Inc., under a cooperative agreement with the National Science Foundation.

³ <http://kurucz.harvard.edu/programs.html>

by Munari et al. (2005). This method offers the advantage that there is no need to identify and measure the equivalent widths of many Fe lines as with the WIDTH9 program.

4.1. Metallicity determinations using the WIDTH program

To determine abundances by this method it is necessary to estimate the stellar parameters T_{eff} and $\text{Log } g$, by means of the Strömgren photometry, for example. With these quantities we adopt the Kurucz (1993)'s model atmosphere appropriated to each star. The model that initially is chosen has solar metallicity. Finally the Kurucz's model together with the measured equivalent widths are used by the WIDTH9 program (Kurucz 1992, 1993) to derive the metallicity.

To obtain T_{eff} and $\text{Log } g$, we have used the $uvby\beta$ mean colors of Hauck & Mermilliod (1998) with two different calibrations: Napiwotzki et al. (1993) and Castelli et al. (1997) and Castelli (1998) (hereafter N93 and C97, respectively), with the TEMPLOGG code (Rogers et al. 1995). This program has been used in the COROT mission preparation (see, for example, Lastennet et al. 2001; Guillon & Magain 2006) and includes reddening corrections, according to Domingo & Figueras (1999) for stars in the range A3–F0, and to Nissen (1988) for spectral types F0–G2.

We have compared the temperatures and gravities derived using both calibrations (N93 and C97) and noticed some differences particularly in the later parameter. For this reason we initially determined metallicities using values derived from both calibrations and later on considered if they significantly affect the final metallicity values. We have also confronted the obtained T_{eff} with those published by Nordström et al. (2004). We found a good agreement in particular with the N93 calibration. With the values of T_{eff} and $\text{Log } g$ derived for each object, we have chosen the corresponding model atmosphere using the Kurucz ATLAS9 (Kurucz 1993) code.

The stellar lines were identified using the general references of *A multiplet table of astrophysical interest* (Moore 1945) and *Wavelengths and transition probabilities for atoms and atomic ions - Part 1: Wavelengths* (Reader et al. 1980), as well as more specialized references for the Fe II lines (Johansson 1978). The equivalent widths were measured by fitting Gaussian profiles through the stellar metallic lines using the IRAS *splot* task. There is no more than a 15% difference among the equivalent widths of the same lines, measured in different spectra. We have excluded from our abundance determinations seriously blended lines.

To determine the abundances we need an initial estimation of the microturbulent velocity (ξ). For this estimation we have used the standard method. We computed the abundances from the Fe lines for a range of possible values of ξ satisfying two conditions: a) that the abundances of Fe lines were not dependent on the equivalent widths and b) that the rms errors were minima. To achieve the first condition the slope in the plot abundance vs ξ must be zero. We tried different ξ values to fulfill this requirement. In this sense the abundance and microturbulent velocity determinations are recursive and simultaneous. Once a ξ value has been fixed the corresponding abundances to all chemical species measured are determined using the WIDTH9 code.

The WIDTH9 code requires the model atmosphere calculated by the ATLAS9 program, the equivalent width of each line as well as atomic constants such as oscillator strength ($\text{Log } gf$) values, excitation potentials, damping constants, etc. In particular for the $\text{Log } gf$ we used Fuhr et al. (1988) and Kurucz (1992). This code calculates the theoretical equivalent widths for an initial

input abundance and compares these values with the measured equivalent widths. Then the code modifies the abundance to achieve a difference between theoretical and measured equivalent widths $< 0.01 \text{ m}\text{\AA}$. The final values of the metallicities corresponding to the N93 and C97 calibrations, are listed in Table 2. We have included the number of lines used in each determination as well as the rms of the average.

To estimate errors for our WIDTH metallicities we consider the following facts. The most significant contribution to the final uncertainties, probably, comes from the equivalent width measurements. We assume a 5% error due to the continuum level determination. This translates into 20% maximum uncertainties in the metallicity estimation. The atomic constants may also have uncertainties. In particular we estimate that the oscillator strength values may cause differences of about 10% in the calculated metallicity. Finally to provide an estimation of "typical" errors introduced by the WIDTH method we increased the T_{eff} by 150 K and the $\text{Log } g$ by 0.15, and recalculated the metallicity value for each star. We derived a median difference of 0.20 dex. The largest difference corresponds to HD 28978 (0.55 dex).

4.2. Metallicity derivations from synthetic spectra: The Downhill method

The WIDTH method is not practical when the number of stars is large. For each object, we need to identify and measure many spectral lines. An alternative would be to compare the observed spectra with a grid of synthetic ones corresponding to different values of the metallicities and choose from the grid the spectrum that better reproduces the observed data (Gray et al. 2001). This comparison has the advantage that the complete profiles of the lines and not only the equivalent widths are used in the metallicity determinations.

In general synthetic spectra depend on four parameters: T_{eff} , surface gravity ($\text{Log } g$), metallicity ($[\text{Fe}/\text{H}]$) and microturbulent velocity (ξ). Following Gray et al. (2001), we applied a multidimensional Downhill Simplex technique, in which the observed spectrum is compared to a grid of synthetic spectra. The "final" synthetic spectrum is an interpolation of spectra, rather than a single point in the grid. As we are working with four variables (T_{eff} , $\text{Log } g$, $[\text{Fe}/\text{H}]$ and ξ) the interpolation is done in 4d, minimizing the square differences in each wavelength (i.e., the χ^2 statistics). The stellar parameters are determined with a higher accuracy than the steps in the grid since they correspond to interpolated values.

The grid of synthetic spectra was taken from Munari et al. (2005). The parameters range covered by the grid is the following:

3500 K $< T_{\text{eff}} < 40000$ K, with steps of 250 K,
 0.0 dex $< \text{Log } g < 5.0$ dex, with steps of 0.5 dex,
 -2.5 dex $< [\text{Fe}/\text{H}] < 0.5$ dex, with steps of 0.5 dex,
 and ξ values of 0, 1, 2, and 4 km/s.

In addition to these parameters, the synthetic spectra are calculated for 15 different rotation velocities, ranging 0 – 500 km/s. In all, Munari et al. (2005)'s library contains 625000 different spectra. These authors calculated the complete synthetic spectral library for four resolving powers: 20000, 11500 (GAIA), 8500 (RAVE) and 2000 (SLOAN). To our request, Dr. U. Munari kindly provided a grid corresponding to the REOSC/CASLEO resolving power (12500).

Synthetic spectral lines were convolved with the instrumental line profile corresponding to the REOSC/CASLEO. Finally they were also convolved with a Gaussian profile corresponding to the rotational velocities of the sample stars, taken from the literature (Glebocki et al. 2000; Mora et al. 2001; Yudin 2001; Royer et al. 2002; Cutispoto et al. 2002, 2003; Pizzolato et al. 2003; Strom et al. 2005; Reiners 2006). We weighted the synthetic spectra by the blaze function of each of the REOSC spectrograph order. Finally we normalized and re-sampled our data to compare them with Munari et al. (2005)'s grid. The spectral sampling of the synthetic spectra is 0.02 Å.

We have implemented the Downhill method (Gray et al. 2001) by means of a Fortran program. From the stellar spectral type or the Strömgren photometry it is possible to estimate "a starting point" in the 4d grid. The Downhill method provides a searching algorithm within the 4d grid and finds the best match, minimizing the χ^2 . In our case, the final spectrum is obtained by an interpolation of 16 spectra of Munari et al. (2005)'s grid. In general it takes 15 – 20 min for each star (50 – 60 iterations) in a Pentium IV 2.0 GHz to find the best interpolated spectrum. Table 3 lists the metallicities obtained with the Downhill method for our sample of Vega-like stars.

To estimate the uncertainties in the metallicities obtained by the Downhill method, we carried out a few tests. We first applied this method to 30 synthetic spectra of known metallicities. The median difference between the derived and known metallicities is 0.2 dex.

The internal consistency of the method has been checked, by fixing one of the four variables and comparing the resultant metallicities. Fixed values for each variable were obtained, for example, from an adopted calibration:

- a) T_{eff} was taken from the N93 calibration,
- b) $\text{Log } g$ was adopted from the N93 calibration,
- c) ξ was fixed at 2.9 km/s, the solar value.

The median difference, calculated by fixing 3 of the 4 variables with respect to the "standard" procedure (i.e., with 4 variable), was 0.05 dex. Considering this value and the median difference derived from the comparison with 30 synthetic spectra of known metallicities (0.2 dex), we estimate a "typical" uncertainty of 0.06 dex for the metallicities derived by the Downhill method.

We have also compared the Downhill method derived metallicities with those obtained by Nordström et al. (2004) and Fischer & Valenti (2005). We first noticed a systematic difference of ~ 0.09 dex between these two determinations. Fischer & Valenti (2005)'s determinations are, on average, larger than those from Nordström et al. (2004)'s. Our Downhill method derived metallicities show a better agreement with Nordström et al. (2004)'s value than with Fischer & Valenti (2005)'s. However this later comparison is based on a relatively small number of common stars.

In the work of Nordström et al. (2004)'s the metallicities are derived as a secondary parameter obtained photometrically. In the case of Fischer & Valenti (2005), the metallicities are obtained by a comparison with synthetic spectra but using only a small range of wavelengths (6000 – 6200 Å). With these limitations in mind, we consider that the external consistency of the Downhill method derived metallicities is acceptable.

We finally mention two parameters taken as fixed by the Downhill method, the radial and the rotational velocities. Radial velocities are initially determined, minimizing the χ^2 with an accuracy of 0.1 km/s or a median value of 0.03 dex in metallicity. Rotational velocities ($v \sin i$) from

Table 4. Medians and dispersions of the metallicities for the Vega-like sample

Method	Median [Fe/H]	Dispersion [Fe/H]	N
WIDTH+N93	-0.14	0.28	113
WIDTH+C97	-0.11	0.26	113
Downhill	-0.11	0.27	113

Note - N93: Napiwotzki et al. (1993)’s calibration; C97: Castelli et al. (1997) and Castelli (1998)’s calibration.

the literature have “typical” dispersions of 5 – 10%, corresponding to an error of about 10% in metallicity.

In summary, we have estimated an internal uncertainty of 0.06 dex for metallicities derived from the Downhill method. A more conservative estimation would indicate a value of 0.1 dex. This corresponds to half of the uncertainty calculated for the WIDTH method (0.2 dex). In this manner, the Downhill method allows a more precise determination of the metallicities for our sample of Vega-like objects.

4.3. Comparison of metallicity determinations by the WIDTH and the Downhill methods

Table 4 lists the medians and the dispersions of the metallicities derived by applying the WIDTH and the Downhill methods for the Vega-like group. In the case of the WIDTH method we present the results corresponding to the two calibrations used (N93 and C97). The derived median values are practically indistinguishable.

Figure 1 compares the metallicity distributions calculated with the WIDTH method plus the N93 calibration (histogram shaded at 0 degree) and the C97 calibrations (histogram shaded at 45 degrees), respectively. The empty histogram shows the distribution derived with the Downhill method for the Vega-like sample. Vertical lines indicate the medians of each distribution. The left line corresponds to the WIDTH+N93 median, and the right line shows (superimposed) the WIDTH+C97 and Downhill medians (see Table 4). The KS-test (Press 1992) indicates that these distributions are similar and represent the same parent population.

We finally adopt the metallicities calculated with the Downhill method for the sample of Vega-like stars, as these determinations use the complete line profiles and not only the equivalent widths. In addition “typical” uncertainties are smaller than those estimated for the WIDTH method.

5. Discussion of the results

The metallicity of the Solar Neighborhood is usually represented by a control sample of stars, which should exclude, in our case, known Vega-like stars. The selection of the control sample is important, because different groups of objects (i.e., stars selected by different criteria) may have different metallicities. For example, Fischer & Valenti (2005) compared two different control samples, with the metallicity distribution of Exoplanet host stars. Their control sets are volume-limited and magnitude-limited. The medians of the metallicity “excess” of the Exoplanet host stars com-

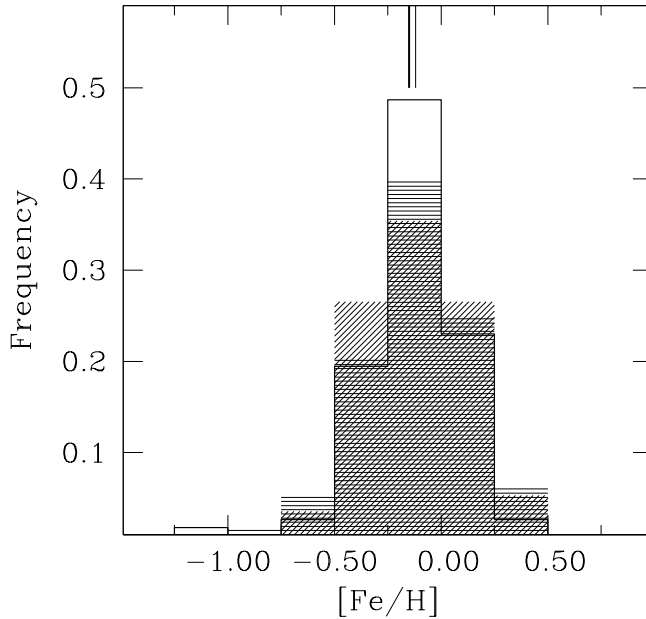


Fig. 1. Metallicity distributions for the Vega-like sample. Histograms shaded at 0 and 45 degrees correspond to the WIDTH method derivations using N93 (Napiwotzki et al. 1993) and C97 (Castelli et al. 1997; Castelli 1998) calibrations, respectively. The empty histogram shows the metallicity distribution derived by the Downhill method. The vertical lines indicate the medians of each distribution. The left line corresponds to the WIDTH+N93 median, and the right line shows (superimposed) the WIDTH+C97 and Downhill medians (see Table 4).

pared with the two groups, are 0.13 and 0.226 dex, respectively. In other words, the "excess" is real, but the amount depends on the control sample used. The two control sets contain different classes of stars. The magnitude-limited sample includes more massive and metal-rich stars than the volume-limited set.

The metallicity distribution of Exoplanet host stars is usually compared with a volume-limited group of solar neighborhood stars (González 1998, 1999; González et al. 2001; Santos et al. 2000, 2003; Santos et al. 2004; Sadakane et al. 2002; Laws et al. 2003). We compared the metallicity distribution of our Vega-like sample with a volume-limited sample of 71 stars, without Doppler detected Exoplanets (Santos et al. 2001; Gilli et al. 2006) and with 98 Exoplanets host stars (Santos et al. 2004). Metallicity values for these two comparison samples were obtained from Nordström et al. (2004). As discussed in Section 4.2, the agreement between our metallicities and those obtained by these authors is acceptable. Figure 2 shows these distributions. Vega-like stars are represented by the empty histogram, stars with planets by the histogram shaded at 0 degree and stars known not to harbor planets detected by the Doppler technique, by the histogram shaded at 45 degrees. The KS test shows no significant difference between the metallicities distributions of the Vega-like stars and stars without planets. On the other hand, the Vega-like stars metallicity distribution is different from the metallicity distribution for stars with planets with a high level of confidence.

Fischer & Valenti (2005) obtained that the probability that a FGK star harbors a giant planet/s increases as $P(Z) \propto (10^Z)^2$, where Z is the stellar metallicity (see also, Wyatt et al. 2007b). If this

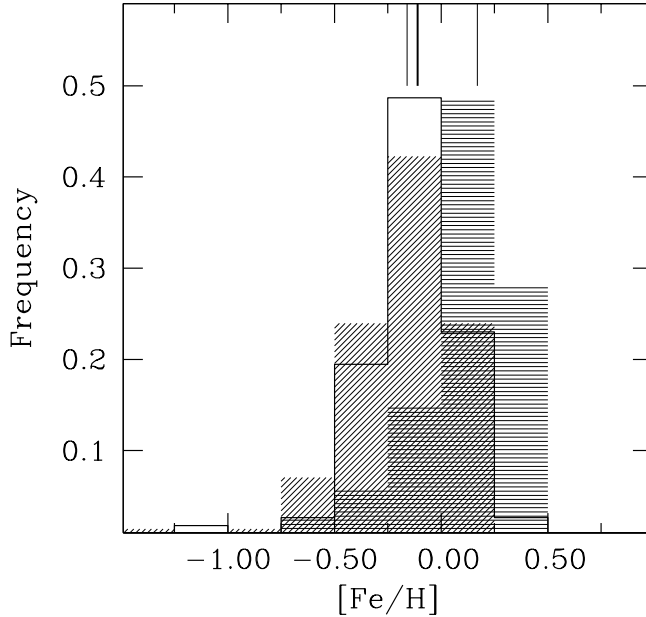


Fig. 2. Metallicity distributions for the Vega-like sample, empty histogram, for stars with planets, histogram shaded at 0 degree, and for stars known not to harbor planets, histogram shaded at 45 degrees. The vertical lines indicate the medians of each distribution: stars without planets, Vega-like stars, and exoplanet host stars, respectively (see Table 5).

relation is also applicable to A stars (the bulge of IRAS detected Vega-like stars), the low median value of the metallicity for the Vega-like group (-0.11 dex, see Table 5) indicates that the probably for these stars to host a planet/s of the type detected by radial velocity surveys is also low. We note, however, that the dispersion of metallicities within the Vega-like stars is also significant (0.26 dex) and at least a fraction of these stars has metallicities high enough to host giant planets, assuming the "excess" of metallicity/presence of a giant planet/s holds for A spectral type stars. In addition it is worthwhile to mention that Doppler searches do not achieve the required precision to detect planets in A stars as metal lines practically disappear.

We also compared the metallicity distribution of Vega-like stars, with a sample of 115 stars without excess at 24 or 70 μm , observed by Spitzer (Beichman et al. 2005, 2006; Bryden et al. 2006; Su et al. 2006). Figure 3 shows these distributions. Vega-like stars are indicated by the empty histogram whereas the stars without excess at 24 or 70 μm are shown by the histogram shaded at 45 degrees. The KS test shows no significant difference between the two distributions. Table 5 lists the medians and the dispersions of the four samples compared in Figures 2 & 3.

The results in Table 5 indicate that, on average, the Vega-like group has metallicities similar to the stars in the Solar Neighborhood without detected planets or disks, in contrast to the Exoplanet host stars group. This result confirms and extends previous works by Greaves et al. (2006) and Chavero et al. (2006), based on relatively small numbers of FG Vega-like stars.

In Figure 4 we analyze the metallicity distribution of Vega-like stars of different spectral types. The number of objects corresponding to each spectral type is indicated between brackets. The vertical bars are the dispersions within the spectral types. A-spectral-type stars still dominate the Vega-like group although Spitzer has significantly contributed with F and G stars during the last

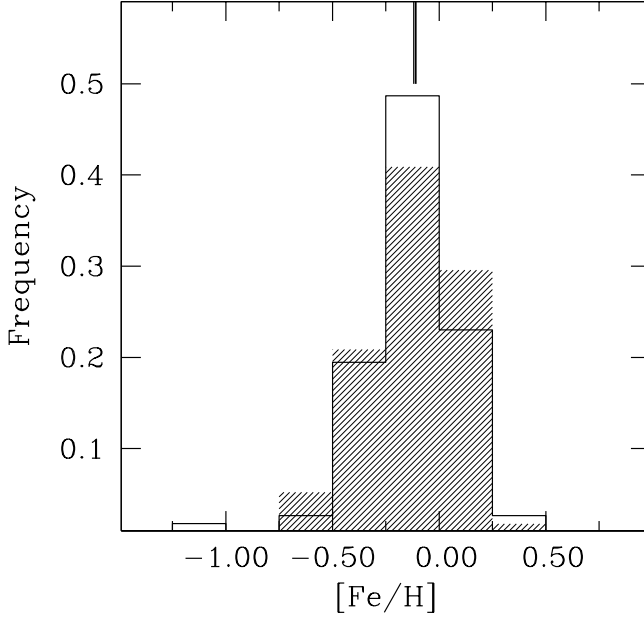


Fig. 3. Metallicity distributions for the Vega-like sample, empty histogram, and for stars without excess at 24 or 70 μm (Beichman et al. 2005, 2006; Bryden et al. 2006; Su et al. 2006). The vertical lines (almost superimposed) indicate the medians of each distribution.

Table 5. Medians and dispersions of the Vega-like sample and three comparison groups

Sample	Median [Fe/H]	Dispersion [Fe/H]	N
Vega-like stars	-0.11	0.27	113
Exoplanet host stars	+0.17	0.22	98
Volume-limited sample without planets	-0.16	0.25	71
Stars without excess at 24 or 70 μm	-0.12	0.24	115

few years (Beichman et al. 2005, 2006; Bryden et al. 2006; Su et al. 2006). Figure 4 shows no trend of the metallicity with the spectral type for the Vega-like group.

As suggested by Greaves et al. (2006) the relatively high metallicity of Exoplanet host stars as well as the solar metallicity value for the Vega-like stars can be understood within the core accumulation model of Pollack et al. (1996). The high metal content of the disk favors the fast formation of giant planets, which needs to accrete an atmosphere and migrate inward before the gas is dissipated from the disk. On the contrary, for Vega-like objects no giant planet needs to be formed and/or migrate inward. The gas may dissipate and still the planetesimal in the external part of the disk may produce dust by collisions.

We tentatively analyzed two small sub-sets of Vega-like objects: the Vega-like stars with planets and the Vega-like group with no Doppler detected planets. The first group is composed of 7 stars: 6 with 70 μm excess detected by Spitzer (HD 33636, HD 50554, HD 52265, HD 82943, HD 128311 and HD 117176; Beichman et al. 2006) and ϵ Eri with infrared and submillimeter excesses (Greaves et al. 1998; Zuckerman 2001). In the second group we include 5 stars without

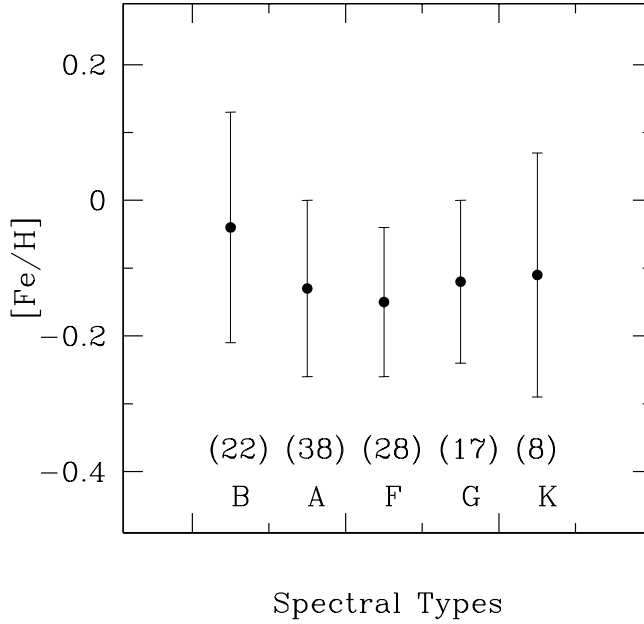


Fig. 4. Metallicity of Vega-like stars of different spectral types. Between brackets is indicated the number of objects in each spectral type bin. The vertical lines are the corresponding dispersions.

Exoplanets detected by the Doppler technique (Santos et al. 2004; Gilli et al. 2006) and showing infrared excess in 24 or 70 μm (HD 7570, HD 38858, HD 69830, HD 76151 and HD 115617; Beichman et al. 2006; Bryden et al. 2006).

The median metallicity of Vega-like stars with planets is +0.07 dex and the dispersion is 0.16 dex. For the Vega-like objects without planets these values are: -0.08 and 0.18 dex, respectively. It seems that when a Vega-like star has a planet the metallicity increases slightly. However the small number of objects available as well as the dispersions prevent us from giving any statistical significance to this initial trend.

Greaves et al. (2007) proposed that the solid-mass (i.e., metals) content in primordial disks, called M_S , is the fundamental parameter that regulates the planet/disk formation. If M_S is small, the star will form a Vega-like disk, while if M_S is larger, a giant planet may be formed. Table 1 of Greaves et al. (2007) shows the range of metallicity and the final configurations (planet+debris, debris, etc.) derived by these authors. The medians of the metallicities of Vega-like stars with and without planets agree with Greaves et al. (2007)'s Table 1. However this can only be considered as an initial trend that needs to be confirmed by increasing the number of Vega-like objects with planets as well as objects known not to harbor Doppler detected planetary mass objects.

6. Summary and Conclusions

We derived spectroscopic metallicities for a group of 113 Southern Hemisphere Vega-like stars. We applied two methods to determine metallicities: the "classical" WIDTH method and a comparison with the grid of synthetic spectra of Munari et al. (2005) by means of the Downhill algorithm. The later method offers the advantage that the complete profile of the line is used in the metallicity

derivation and not only the equivalent width. In addition we estimated smaller uncertainties in the metallicities derived by the Downhill method (0.1 dex) than with the WIDTH code (0.2 dex).

Vega-like stars have metallicities similar to Solar Neighborhood stars without planets or disks and significantly different from the Exoplanet host stars. This result confirms previous estimations by Greaves et al. (2006) and Chavero et al. (2006), based on comparatively smaller samples.

The low metallicities for the Vega-like group (median = -11 dex) in relation to the Exoplanet host stars (median = $+0.17$, see for example, Fischer & Valenti 2005), may indicate that the probability for these stars to host a planet/s of the type detected by radial velocity surveys is also low. However the dispersion of metallicities within the Vega-like stars is also significant (0.26 dex) and thus a fraction of these objects may have metallicities high enough to form giant planets. We caution that Exoplanet host stars are mainly of FGK spectral types whereas the bulge of IRAS detected Vega-like stars has A spectral type which are, in general, excluded from radial velocity searches since high precisions are not feasible. In this we are assuming that the probability of a A star to be associated with a giant planet depends on the metallicity as is the case for FGK stars.

We find no trend in the metallicities of Vega-like objects with the spectral type. Greaves et al. (2006) suggestion make compatible the relative high metallicity of Exoplanet host stars and the solar Neighborhood value for Vega-like stars with the core accumulation model of Pollack et al. (1996).

Analyzing two relatively small sub-samples, we find that Vega-like stars with a Doppler detected planet have slightly higher metallicities than Vega-like stars known not to harbor such a planet. However this must be considered only as an initial trend that needs to be confirmed by increasing both samples to achieve a statistical significant result.

Acknowledgements. The authors thank Drs. F. Castelli, P. Bonifacio and L. Sbordone for making their codes available to them.

References

- Aumann, H. H., Beichman, C. A., Gillett, F. C., de Jong, T., Houck, J. R., Low, F. J., Neugebauer, G., Walker, R. G., & Wesselius, P. R. 1984, *ApJ*, 278, 23
- Apai, D., Janson, M., Moro-Martin, A., Meyer, M. R., Mamajek, E. E., Masciadri, E., Henning, Th., Pascucci, I., Kim, J. S., Hillenbrand, L. A., et al. 2008, *ApJ*, 672, 1196
- Backman, D. E. & Paresce, F. 1993, in *Protostars and planets III*, ed. Levy, Lunine, Mathews (Tucson: Univ. Arizona Press), 1253
- Beichman, C. A., Bryden, G., Rieke, G. H., Stansberry, J. A., Trilling, D. E., Stapelfeldt, K. R., Werner, M. W., Engelbracht, C. W., Blaylock, M., Gordon, K. D., et al. 2005, *ApJ*, 622, 1160
- Beichman, C. A., Bryden, G., Stapelfeldt, K. R., Gautier, T. N., Grogan, K., Shao, M., Velusamy, T., Lawler, S. M., Blaylock, M., Rieke, G. H., et al. 2006, *ApJ*, 652, 1674
- Beichman, C. A., Tanner, A., Bryden, G., Stapelfeldt, K. R., Werner, M. W., Rieke, G. H., Trilling, D. E., Lawler, S., & Gautier, T. N., 2006, *ApJ*, 639, 1166
- Bryden, G., Beichman, C. A., Trilling, D. E., Rieke, G. H., Holmes, E. K., Lawler, S. M., Stapelfeldt, K. R., Werner, M. W., Gautier, T. N., Blaylock, M. et al. 2006, *ApJ*, 636, 1098
- Castelli, F., Gratton, R. G., & Kurucz, R. L. 1997, *A&A*, 318, 841
- Castelli, F. 1998, *Memorie della Societa Astronomia Italiana*, 69, 165
- Chavero, C., Gómez, M., Whitney, B. A., & Saffe, C. 2006, *A&A*, 452, 921
- Chen, C. H., Patten, B. M., Werner, M. W., Dowell, C. D., Stapelfeldt, K. R., Song, I., Stauffer, J. R., Blaylock, M., Gordon, K. D., & Krause, V. 2005, *ApJ*, 634, 1372

- Chen, C. H., Sargent, B. A., Bohac, C., Kim, K. H., Leibensperger, E., Jura, M., Najita, J., Forrest, W. J., Watson, D. M., Sloan, G. C., & Keller, L. D. 2006, *ApJS*, 166, 351
- Cheng, K. P., Bruhweiler, F. C., Kondo, Y., & Grady, C. A. 1992, *ApJ*, 396, 83
- Clampin, M., Krist, J. E., Ardila, D. R., Golimowski, D. A., Hartig, G. F., Ford, H. C., Illingworth, G. D., Bartko, F., Benítez, N., Blakeslee, J. P., et al. 2003, *AJ*, 126, 385
- Cote, J., 1987, *A&A*, 181, 77
- Cutispoto, G., Pastori, L., Pasquini, L., de Medeiros, J. R., Tagliaferri, G., & Andersen, J. 2002, *A&A*, 384, 491
- Cutispoto, G., Tagliaferri, G., de Medeiros, J. R., Pastori, L., Pasquini, L., & Andersen, J. 2003, *A&A*, 397, 987
- Decin, G., Dominik, C., Waters, L. B. F. M., & Waelkens, C. 2003, *ApJ*, 598, 636
- Fajardo-Acosta, S. B., Stencel, R. E., Backman, D. E., & Thakur, N. 1999, *ApJ*, 520, 215
- Fischer, D. A., & Valenti, J. A. 2005, *ApJS*, 622, 1102
- Friedemann, C., Guertler, J., & Loewe, M. 1996, *A&AS* 117, 205
- Fuhr, J. R., Martin, G. A., & Wiese, W. L. 1988, *Atomic transition probabilities, Scandium through Manganese*, New York: American Institute of Physics (AIP) and American Chemical Society
- Gillett, F. C. 1986, in *Light on dark matter; Proceedings of the First Infra-Red Astronomical Satellite Conference*, Noordwijk, Netherlands, June 10-14, 1985 (A87-11851 02-90). Dordrecht, D. Reidel Publishing Co., 61
- Gillon, M., & Magain, P. 2006, *A&A*, 448, 341
- Domingo, A., & Figueras, F. 1999, *A&A*, 343, 446
- Gilli, G., Israelian, G., Ecuivillon, A., Santos, N. C., & Mayor, M. 2006, *A&A*, 449, 723
- Glebocki, R., & Stawikowski, A. 2000, *Acta Astron.*, 50, 509
- González, G. 1998, *A&A*, 334, 221
- González, G. 1999, *MNRAS*, 308, 447
- González, G., Laws, C., Tyagi, S., & Reddy, B. E. 2001, *AJ*, 121, 432
- Gray, R. O., Graham, P. W., & Hoyt, S. R. 2001, *AJ*, 121, 2159
- Greaves, J. S., Holland, W. S., Moriarty-Schieven, G., Jenness, T., Dent, W. R. F., Zuckerman, B., McCarthy, C., Webb, R. A., Butner, H. M., Gear, W. K., & Walker, H. J. 1998, *ApJ*, 506, 133
- Greaves, J. S., Fischer, D. A., & Wyatt, M. C. 2006, *MNRAS*, 366, 283
- Greaves, J. S., Fischer, D. A., Wyatt, M. C., Beichman, C. A., & Bryden, G. 2007, *MNRAS*, 378, L1
- Habing, H. J., Dominik, C., Jourdain de Muizon, M., Laureijs, R. J., Kessler, M. F., Leech, K., Metcalfe, L., Salama, A., Siebenmorgen, R., Trams, N., & Bouchet, P. 2001, *A&A*, 365, 545
- Hauck, B., & Mermilliod, M. 1998, *A&AS*, 129, 431
- Hillenbrand, L. A., Carpenter, J. M., Kim, J. S., Meyer, M. R., Backman, D. E., Moro-Martín, A., Hollenbach, D. J., Hines, D. C., Pascucci, I., & Bouwman, J. 2008, *ApJ*, 677, 630
- Holland, W. S., Greaves, J. S., Zuckerman, B., Webb, R. A., McCarthy, C., Coulson, I. M., Walther, D. M., Dent, W. R. F., Gear, W. K., & Robson, I. 1998, *Nature*, 392, 788
- Jaschek, M., Jaschek, C., & Egret, D. 1986, *A&A*, 158, 325
- Johansson S. 1978, *Phys. Scripta*, 18, 217
- Jura, M., Chen, C. H., Furlan, E., Green, J., Sargent, B., Forrest, W. J., Watson, D. M., Barry, D. J., Hall, P., Herter, T. L., et al. 2004, *ApJS*, 154, 453
- Kim, J. S., Hines, D. C., Backman, D. E., Hillenbrand, L. A., Meyer, M. R., Rodmann, J., Moro-Martín, A., Carpenter, J. M., Silverstone, M. D., & Bouwman, J. 2005, *A&A*, 632, 659
- Kurucz, R. L. 1992, *Rev. Mexicana Astron. Astrofis.*, 23, 45
- Kurucz, R. L. 1993, *ATLAS) Stellar Atmosphere Programs and 2 km/s grid*, Kurucz CM-ROM No. 13, Smithsonian Astrophysical Observatory, Cambridge, MA
- Lastennet, E., Lignies, F., Buser, R., Lejeune, T., Lftinger, T., Cuisinier, F., & van't Veer-Menneret, C. 2001, *The Journal of Astronomical Data* Vol. 7
- Laureijs, R. J., Jourdain de Muizon, M., Leech, K., Siebenmorgen, R., Dominik, C., Habing, H. J., Trams, N., & Kessler, M. F. 2002, *A&A*, 387, 285
- Laws, C., González, G., Walker, K. M., Tyagi, S., Dodsworth, J., Snider, K., & Suntzeff, N. B. 2003, *AJ*, 125, 2664
- Mamajek, E. E., Hines, D. C., Backman, D. E., Bouwman, J., Hillenbrand, L. A., Carpenter, J. M., Meyer, M. R., Kim, J. S., Silverstone, M. D., Rodmann, J. et al., 2005, *A&AS*, 207, 6348
- Mannings, V., & Barlow, M. J. 1998, *ApJ*, 497, 330

- Meyer, M. R., Hillenbrand, L. A., Backman, D. E., Beckwith, S. V. W., Bouwman, J., Brooke, T. Y., Carpenter, J. M., Cohen, M., Gorti, U., Henning, T. et al. 2004, *ApJS*, 154, 422
- Moore, C. E. 1945, *A multiplet table of astrophysical interest* Princeton, N.J., The Observatory, 1945. Rev. ed.
- Mora, A., Merín, B., Solano, E., Montesinos, B., de Winter, D., Eiroa, C., Ferlet, R., Grady, C. A., Davies, J. K., Miranda, L. F. et al. 2001, *A&A*, 378, 116
- Munari, U., Sordo, R., Castelli, F., & Zwitter, T. 2005, *A&A*, 442, 1127
- Napiwotzki, R., Schoenberner, D., & Wenske, V. 1993, *A&A*, 268, 653
- Nissen, P. E. 1988, *A&A*, 199, 146
- Nordström, B., Mayor, M., Andersen, J., Holmberg, J., Pont, F., Jorgensen, B. R., Olsen, E. H., Udry, S., & Mowlavi, N. 2004, *A&A*, 418, 989
- Oudmajer, R. D., van der Veen, W. E. C. J., Waters, L. B. F. M., Trams, N. R., Waelkens, C., & Engelsman, E. 1992, *A&AS* 96, 625
- Pascucci, I., Gorti, U., Hollenbach, D., Najita, J., Meyer, M. R., Carpenter, J. M., Hillenbrand, L. A., Herczeg, G. J., Padgett, D. L., Mamajek, E. E., et al. 2006, *ApJ*, 651, 1177
- Pasquini, L., Döllinger, M. P., Weiss, A., Girardi, L., Chavero, C., Hatzes, A. P., da Silva, L., & Setiawan, J. 2007, *A&A*, 473, 979
- Patten, B. M., & Willson, L. A. 1991, *AJ*, 102, 323
- Pizzolato, N., Maggio, A., Micela, G., Sciortino, S., & Ventura, P. 2003, *A&A*, 397, 147
- Press W. H., Teukolsky S. A., Vetterling W. T., & Flannery B. P. 1992, *Numerical Recipes in Fortran: The Art of Scientific Computing*, Cambridge University Press, 2nd edition, p. 617
- Pollack, J. B., Hubickyj, O., Bodenheimer, P., Lissauer, J. J., Podolak, M., & Greenzweig, Y. 1996, *Icarus*, 124, 62
- Reader, J., Corliss, C. H., Wiese, W. L., & Martin, G. A. 1980, *Wavelengths and transition probabilities for atoms and atomic ions - Part 1: Wavelengths* National Standard Reference Data Series (NSRDS-NBS), Washington: National Bureau of Standards (NBS)
- Reiners, A. 2006, *A&A*, 446, 267
- Rieke, G. H., Su, K. Y. L., Stansberry, J. A., Trilling, D., Bryden, G., Muzerolle, J., White, B., Gorlova, N., Young, E. T., Beichman, C. A. et al. 2005, *ApJ*, 620, 1010
- Rogers, N. Y. 1995, *Comm. in Asteroseismology* 78
- Royer, F., Gerbaldi, M., Faraggiana, R., & Gómez, A. E. 2002, *A&A*, 381, 105
- Sadakane, K., & Nishida, M. 1986, *PASP*, 98, 685
- Sadakane, K., Ohkubo, M., Takeda, Y., Sato, B., Kambe, E., & Aoki, W. 2002, *PASJ*, 54, 911
- Santos, N. C., Israelian, G., & Mayor, M. 2000, *A&A*, 363, 228
- Santos, N. C., Israelian, G., & Mayor, M. 2001, *A&A*, 373, 1019
- Santos, N. C., Israelian, G., & Mayor, M. Rebolo, R., & Udry, S. 2003, *A&A*, 398, 363
- Santos, N. C., Israelian, G., & Mayor, M. 2004, *A&A*, 415, 1153
- Schneider, G., Silverstone, M. D., Hines, D. C., Augereau, J.-C., Pinte, C., Menard, F., Krist, J., Clampin, M., Grady, C., Golimowski, D., et al. 2006, *ApJ*, 650, 414
- Sheret, I., Ramsay Howat, S. K., & Dent, W. R. F. 2003, *MNRAS*, 343, 65
- Sheret, I., Dent, W. R. F., & Wyatt, M. C. 2004, *MNRAS*, 348, 128
- Silverstone, M. D., Meyer, M. R., Mamajek, E. E., Hines, D. C., Hillenbrand, L. A., Najita, J., Pascucci, I., Bouwman, J., Kim, J. S., Carpenter, J. M. et al. 2006, *ApJ*, 639, 1138
- Stencel, R. E., & Backman, D. E. 1991, *ApJS*, 75, 905
- Song, I., Caillault, J.-P., Barrado y Navascués, D., & Stauffer, J. R. 2001, *ApJ*, 546, 352
- Strom, S. E., Wolff, S. C., & Dror, D. H. A. 2005, *ApJ*, 129, 809
- Su, K. Y. L., Rieke, G. H., Stansberry, J. A., Bryden, G., Stapelfeldt, K. R., Trilling, D. E., Muzerolle, J., Beichman, C. A., Moro-Martin, A., Hines, D. C., & Werner, M. W. 2006, *ApJ*, 653, 675
- Sylvester, R. J., Skinner, C. J., Barlow, M. J., & Mannings, V. 1996, *MNRAS*, 279, 915
- Sylvester, R. J. & Mannings, V. 2000, *MNRAS*, 313, 73
- Telesco, C. M., Fisher, R. S., Piña, R. K., Knacke, R. F., Dermott, S. F., Wyatt, M. C., Grogan, K., Holmes, E. K., Ghez, A. M., Prato, L., et al. 2000, *ApJ*, 530, 329
- Trilling, D. E., Bryden, G., Beichman, C. A., Rieke, G. H., Su, K. Y. L., Stansberry, J. A., Blaylock, M., Stapelfeldt, K. R., Beeman, J. W., & Haller, E. E. 2008, *ApJ*, 674, 1086

- Uzpen, B., Kobulnicky, H. A., Olsen, K. A. G., Clemens, D. P., Laurance, T. L., Meade, M. R., Babler, B. L., Indebetouw, R., Whitney, B. A., Watson, C. et al. 2005, *ApJ*, 629, 512
- Walker, H. J., & Wolstencroft, R. D. 1988, *PASP*, 100, 1509
- Waters, L. B. F. M., van den Ancker, M. E., Baas, F., van der Bliek, N. S., Bontekoe, T. R., Geballe, T. R., Grady, C. A., Kester, D. J. M., Oudmaijer, R. D., & Sandell, G. 1995, *A&A*, 299, 173
- Wyatt, M. C., Smith, R., Su, K. Y. L., Rieke, G. H., Greaves, J. S., Beichman, C. A., & Bryden, G. 2007a, *ApJ*, 663, 365
- Wyatt, M. C., Clarke, C. J., & Greaves, J. S. 2007b, *MNRAS*, 380, 1737
- Yudin, R. V. 2001, *A&A*, 368, 912
- Zuckerman, B. 2001, *A&A Rev.*, 39, 549

Table 1. Sample of Vega-like stars observed at the CASLEO

Star	Distance [pc]	V	Spectral Type	Reference
HD 105	40	7.51	G0V	DEC03 HILL08
HD 142	26	5.70	G1V	BE05 TR08
HD 2623	365	7.93	K2	SB91
HD 3003	46	5.07	A0V	MB98 O92 SB91 WY07
HD 9672	61	5.62	A1V	MB98 O92 SB91 PW91 WW88 SN86 WY07
HD 10647	17	5.52	F8V	MB98 O92 SB91 DEC03 TR08
HD 10700	4	3.49	G8V	MB98 HDJL01 DEC03
HD 10800	27	5.88	G2V	MB98 BE06 BR06
HD 17206	14	4.47	F5V	O92 SB91
HD 17848	51	5.25	A2V	MB98
HD 18978	26	4.08	A4V	SCBS01
HD 20010	14	3.80	F8V	O92 WW88
HD 20794	6	4.26	G8V	DEC03 BE06
HD 21563	182	6.14	A4V	MB98
HD 22049	3	3.72	K2V	SB91 WW88 HDJL01 DEC03
HD 22484	14	4.29	F9V	DEC03 TR08
HD 23362	309	7.91	K2	SB91
HD 25457	19	5.38	F5V	DEC03 PAS06 HILL08
HD 28375	118	5.53	B3V	O92 SB91 TR08
HD 28978	125	5.67	A2V	BP93
HD 30495	13	5.49	G3V	HDJL01 DEC03 TR08
HD 31295	37	4.64	A0V	SN86 WY07
HD 33262	12	4.71	F7V	BR06 TR08
HD 33636	29	7.00	G0	BE05 TR08
HD 33949	172	4.36	B7V	MB98 O92 SB91 PW91 SN86
HD 35850	27	6.30	F7V	DEC03 PAS06 AP08
HD 36267	88	4.20	B5V	BP93
HD 37484	60	7.26	F3V	PAS06 HILL08
HD 38206	69	5.73	A0V	MB98 DEC03 WY07
HD 38385	53	6.25	F3V	MB98
HD 38393	9	3.59	F7V	MB98 HDJL01 SH03 BE06
HD 38678	22	3.55	A2V	MB98 O92 PW91 AP91 C87 HDJL01 DEC03 SU06 WY07
HD 39014	44	4.34	A7V	O92 SB91 C87 JU04
HD 39060	19	3.85	A3V	MB98 O92 C92 SB91 PW91 AP91 WW88 C87 JJE86 HDJL01 DEC03 WY07
HD 40136	15	3.71	F1V	MB98 BE06b
HD 41700	27	6.35	G0V	DEC03 HILL08
HD 41742	27	5.93	F4V	MB98
HD 43955	305	5.51	B3V	MB98

Table 1. Continued.

Star	Distance [pc]	V	Spectral Type	Reference
HD 66591	166	4.81	B3V	MB98
HD 68456	21	4.74	F5V	BR06 TR08
HD 69830	13	5.95	K0V	MB98 BE06 BR06
HD 71043	73	5.89	A0V	WY07
HD 71155	38	3.91	A0V	PW91 C87 WY07
HD 75416	97	5.46	B9V	MB98 SU06 WY07
HD 76151	17	6.01	G3V	BE06 BR06
HD 79108	115	6.14	A0V	WY07
HD 80950	81	5.86	A0V	MB98 WY07
HD 82943	27	6.54	G0	BE05 TR08
HD 86087	98	5.71	A0V	BP93
HD 88955	32	3.85	A2V	MB98
HD 98800	47	8.89	K4V	MB98 SB91 WW88 MA05
HD 99211	26	4.06	A9V	MB98
HD 102647	11	2.14	A3V	O92 C92 SB91 PW91 WW88 C87 HDJL01 DEC03
HD 105211	20	4.14	F2	BE06b
HD 105686	101	6.16	A0V	MB98
HD 108257	123	4.82	B3Vn	BP93
HD 108483	136	3.91	B3V	MB98
HD 109085	18	4.30	F2V	MB98 SB91 SH03 BE06b
HD 109573	67	5.78	A0V	TE00
HD 111786	60	6.14	A0	WY07
HD 113766	131	7.48	F5V	MB98 O92 CH06
HD 115617	9	4.74	G5V	BR06
HD 115892	18	2.75	A2V	MB98 SU06 WY07
HD 117176	18	4.97	G5V	BE05 BR06
HD 117360	35	6.52	F6V	MB98
HD 121847	104	5.20	B8V	MB98 PW91
HD 123160		8.66	K5	SB91
HD 124771	169	5.06	B4V	MB98
HD 128311	17	7.48	K0	BE05 BE06
HD 131885	121	6.91	A0V	MB98
HD 135344	78	7.91	F3V	MB98 O92 WW88
HD 136246	143	7.18	A1V	WY07
HD 139365	136	3.66	B2.5V	MB98
HD 139664	18	4.64	F5V	O92 PW91 WW88 HDJL01 DEC03 CH06 BE06b
HD 141569	99	7.11	B9	O92 SB91 WW88 JJE86 SH03 CL03
HD 142096	109	5.04	B3V	MB98 O92 SB91
HD 142114	133	4.59	B2.5V	MB98 O92

Table 1. Continued.

Star	Distance [pc]	V	Spectral Type	Reference
HD 142165	127	5.38	B5V	MB98
HD 144432	253	8.19	F0V	MB98 O92 WW88
HD 145482	143	4.58	B2V	MB98
HD 150638	240	6.46	B8V	PW91
HD 152391	17	6.65	G8V	DEC03 BR06 TR08
HD 158643	131	4.78	A0V	O92
HD 158793		8.83		BP93
HD 159082	152	6.42	B9.5V	BP93
HD 160691	15	5.12	G5V	MB98 BE05
HD 161868	29	3.75	A0V	O92 C87 SN86
HD 164249	47	7.01	F5V	PW91 DEC03
HD 164577	81	4.42	A2V	WA95
HD 165341	5	4.03	K0V	DEC03
HD 166841	214	6.32	B9V	MB98
HD 169830	36	5.90	F8V	BE05
HD 176638	56	4.74	A0V	MB98
HD 177817	274	6.00	B7V	DEC03
HD 178253	40	4.11	A0V	MB98 PW91
HD 181296	48	5.03	A0V	BP93 MB98
HD 181327	51	7.04	F6V	MB98 SCH06 CH06
HD 181869	52	3.96	B8V	MB98 WY07
HD 183324	59	5.79	A0V	WY07
HD 185507	209	5.18	B3V	BP93 FR96
HD 188228	33	3.97	A0V	SU06
HD 191089	54	7.18	F5V	MB98 HILL08 CH06
HD 198160	73	5.67	A2	RI05
HD 199260	21	5.70	F7V	BE06b
HD 203608	9	4.21	F6V	MB98 BE06 BR06
HD 206893	39	6.69	F5V	DEC03
HD 207129	16	5.57	G2V	MB98 O92 WW88 O86 HDJL01 DEC03 SH03 TR08
HD 209253	30	6.63	F7V	DEC03 PAS06 HILL08
HD 216435	33	6.03	G3V	BP93
HD 216437	27	6.04	G4V	BE06 BR06
HD 216956	8	1.17	A3V	MB98 O92 C92 SB91 WW88 C87 HDJL01 DEC03 HO98
HD 221853	71	7.35	F0	DEC03
HD 224392	49	5.00	A1V	MB98 O92

Note - The distances, visual magnitudes and spectral types are taken from the Hipparcos catalog.

References (alphabetically sorted): AP08 = Apai et al. (2008), BE05 = Beichman et al. (2005), BE06 = Beichman et al. (2006), BE06b = Beichman et al. (2006b), BP93 = Backman & Paresce (1993), BR06 = Bryden et al. (2006), C87 = Cote (1987), C92 = Cheng et al. (1992), CH06 = Chen et al. (2006), CL03 = Clampin et al. (2003), DEC03 = Decin et al. (2003), FR96 = Friedemann et al. (1996), HDJL01 = Habing et al. (2001), HILL08 = Hillenbrand et al. (2008), HO98 = Holland et al. (1998), JJE86 = Jaschek et al. (1986), JU04 = Jura et al. (2004), MA05 = Mamajek et al. (2005), MB98 = Mannings & Barlow (1998), O92 = Oudmaijer et al. (1992), PAS06 = Pascucci et al. (2006), PW91 = Patten & Willson (1991), RI05 = Rieke et al. (2005), SB91 = Stencel & Backman (1991), SCBS01 = Song et al. (2001), SH03 = Sheret et al. (2003), SCH06 = Schneider et al. (2006), SN86 = Sadakane & Nishida (1986), SU06 = Su et al. (2006), TE00 = Telesco et al. (2000), TR08 = Trilling et al. (2008), WA95 = Waters et al. (1995), WW88 = Walker & Wolstencroft (1988), WY07 = Wyatt et al. (2007a).

Table 2. Metallicities, dispersion (δ) and number of lines (N) used with the WIDTH9 program, applying the N93 and C97 calibrations for the Vega-like sample

Star	N93	N93	C97	C97	N
	[Fe/H]	δ [Fe/H]	[Fe/H]	δ [Fe/H]	
HD 105	-0.37	0.26	-0.33	0.26	15
HD 142	-0.45	0.27	-0.27	0.25	20
HD 2623	-0.20	0.26	0.09	0.20	23
HD 3003	0.17	0.22	0.07	0.31	17
HD 9672	-0.32	0.26	-0.31	0.21	24
HD 10647	0.12	0.22	-0.07	0.28	29
HD 10700	-0.73	0.29	-0.67	0.23	17
HD 10800	0.16	0.27	0.12	0.26	30
HD 17206	-0.22	0.27	0.03	0.21	22
HD 17848	-0.02	0.28	-0.17	0.20	21
HD 18978	-0.39	0.25	-0.11	0.23	22
HD 20010	-0.64	0.20	-0.62	0.30	27
HD 20794	-0.17	0.29	-0.58	0.24	17
HD 21563	-0.41	0.30	-0.10	0.26	19
HD 22049	-0.08	0.25	-0.13	0.27	22
HD 22484	-0.22	0.28	-0.19	0.26	21
HD 23362	-0.07	0.25	-0.47	0.29	25
HD 25457	0.18	0.21	-0.22	0.22	29
HD 28375	0.10	0.29	-0.19	0.26	23
HD 28978	0.20	0.22	0.33	0.24	18
HD 30495	0.11	0.29	0.13	0.24	23
HD 31295	-0.68	0.24	-0.76	0.25	27
HD 33262	0.07	0.25	-0.09	0.24	27
HD 33636	0.03	0.20	-0.09	0.27	16
HD 33949	0.00	0.21	-0.23	0.27	19
HD 35850	-0.23	0.27	-0.12	0.24	26
HD 36267	-0.23	0.23	-0.02	0.23	21
HD 37484	-0.17	0.31	-0.25	0.30	28
HD 38206	-0.06	0.21	0.32	0.23	23
HD 38385	0.09	0.25	0.12	0.30	24
HD 38393	0.30	0.21	0.21	0.27	26
HD 38678	-0.13	0.21	-0.35	0.28	29
HD 39014	-0.41	0.26	-0.39	0.30	23
HD 39060	0.00	0.29	0.17	0.21	16
HD 40136	-0.27	0.30	-0.33	0.27	29
HD 41700	-0.14	0.22	-0.41	0.22	23
HD 41742	-0.31	0.28	-0.30	0.30	16

Table 2. Continued.

Star	[Fe/H]	δ [Fe/H]	[Fe/H]	δ [Fe/H]	N
HD 43955	-0.15	0.26	-0.20	0.26	21
HD 66591	0.04	0.25	-0.09	0.21	23
HD 68456	-0.36	0.26	-0.20	0.24	21
HD 69830	-0.07	0.23	-0.06	0.29	24
HD 71043	0.19	0.25	-0.14	0.25	23
HD 71155	-0.11	0.26	0.25	0.21	21
HD 75416	0.10	0.28	0.01	0.26	24
HD 76151	-0.07	0.26	-0.07	0.22	22
HD 79108	-0.10	0.28	-0.26	0.22	16
HD 80950	-0.29	0.31	-0.28	0.20	18
HD 82943	0.35	0.30	0.32	0.22	28
HD 86087	0.27	0.24	-0.07	0.28	29
HD 88955	-0.14	0.30	0.12	0.29	16
HD 98800	-0.05	0.25	-0.24	0.23	23
HD 99211	-0.15	0.25	0.14	0.23	26
HD 102647	-0.24	0.20	-0.07	0.27	27
HD 105211	-0.36	0.22	-0.04	0.26	18
HD 105686	-0.72	0.29	-0.39	0.27	13
HD 108257	-0.38	0.24	-0.36	0.21	16
HD 108483	0.02	0.21	0.14	0.25	20
HD 109085	-0.20	0.24	-0.23	0.27	20
HD 109573	-0.06	0.31	0.10	0.30	15
HD 111786	-1.42	0.30	-1.65	0.22	24
HD 113766	0.06	0.23	-0.14	0.27	16
HD 115617	0.20	0.29	0.13	0.24	16
HD 115892	-0.29	0.27	-0.33	0.28	14
HD 117176	0.01	0.26	-0.12	0.26	25
HD 117360	-0.39	0.21	-0.61	0.26	25
HD 121847	-0.30	0.26	0.10	0.27	16
HD 123160	0.27	0.27	0.17	0.25	28
HD 124771	0.15	0.21	0.01	0.21	29
HD 128311	0.16	0.24	0.04	0.29	16
HD 131885	-0.44	0.29	-0.19	0.28	23
HD 135344	-0.37	0.21	-0.41	0.28	20
HD 136246	-0.29	0.23	-0.49	0.28	27
HD 139365	0.02	0.25	0.35	0.29	26
HD 139664	-0.46	0.28	-0.08	0.26	24
HD 141569	-0.32	0.27	-0.01	0.20	18
HD 142096	-0.28	0.28	-0.16	0.23	14
HD 142114	0.09	0.26	0.06	0.26	21

Table 2. Continued.

Star	[Fe/H]	δ [Fe/H]	[Fe/H]	δ [Fe/H]	N
HD 142165	-0.03	0.23	0.10	0.30	20
HD 144432	-0.19	0.23	-0.13	0.28	25
HD 145482	-0.38	0.27	-0.19	0.25	20
HD 150638	-0.34	0.23	-0.52	0.22	22
HD 152391	-0.24	0.26	-0.26	0.31	27
HD 158643	-0.44	0.22	-0.20	0.30	26
HD 158793	0.25	0.25	0.37	0.24	16
HD 159082	0.09	0.31	-0.22	0.24	26
HD 160691	-0.07	0.25	-0.06	0.21	21
HD 161868	0.11	0.30	-0.26	0.28	26
HD 164249	-0.04	0.22	-0.04	0.23	29
HD 164577	-0.14	0.24	-0.37	0.24	24
HD 165341	-0.26	0.30	-0.38	0.26	26
HD 166841	-0.16	0.31	0.05	0.27	16
HD 169830	-0.15	0.23	0.31	0.25	26
HD 176638	-0.21	0.23	-0.05	0.28	21
HD 177817	0.13	0.27	0.04	0.21	26
HD 178253	0.12	0.23	-0.26	0.22	23
HD 181296	0.06	0.30	0.14	0.28	21
HD 181327	0.34	0.23	0.24	0.28	27
HD 181869	-0.02	0.28	-0.03	0.29	19
HD 183324	-1.13	0.27	-1.29	0.30	21
HD 185507	-0.14	0.27	-0.07	0.21	31
HD 188228	-0.17	0.25	-0.02	0.31	17
HD 191089	-0.41	0.25	-0.17	0.29	24
HD 198160	-0.78	0.29	-0.99	0.24	25
HD 199260	-0.26	0.28	-0.01	0.31	18
HD 203608	-0.43	0.28	-0.72	0.24	19
HD 206893	-0.07	0.27	0.20	0.23	24
HD 207129	-0.26	0.20	-0.22	0.27	26
HD 209253	0.02	0.27	-0.26	0.26	16
HD 216435	0.07	0.26	-0.17	0.25	22
HD 216437	0.34	0.21	0.27	0.28	21
HD 216956	-0.42	0.28	-0.22	0.20	22
HD 221853	-0.18	0.24	0.08	0.26	15
HD 224392	0.09	0.21	0.14	0.27	23

Table 3. T_{eff} , $\text{Log } g$ and $[\text{Fe}/\text{H}]$ derived using the Downhill method, for the sample of Vega-like stars

Star	T_{eff} [K]	$\text{Log } g$	$[\text{Fe}/\text{H}]$
HD 105	5989	4.57	-0.13
HD 142	6182	4.12	-0.21
HD 2623	4923	4.10	-0.15
HD 3003	8794	4.10	0.06
HD 9672	8865	4.21	-0.12
HD 10647	5954	4.67	-0.01
HD 10700	5499	4.97	-0.53
HD 10800	5901	4.84	0.09
HD 17206	6359	4.57	-0.14
HD 17848	8308	3.96	-0.05
HD 18978	8050	4.14	-0.25
HD 20010	6072	4.07	-0.39
HD 20794	5629	4.70	-0.35
HD 21563	6714	4.22	-0.25
HD 22049	4963	3.92	-0.17
HD 22484	5943	4.29	-0.17
HD 23362	4899	4.21	-0.23
HD 25457	6364	4.68	0.00
HD 28375	15275	4.20	-0.02
HD 28978	9075	4.26	0.17
HD 30495	5759	4.53	0.01
HD 31295	8651	4.11	-0.75
HD 33262	6073	4.83	-0.10
HD 33636	5744	4.56	-0.08
HD 33949	12459	3.44	-0.07
HD 35850	6021	4.66	-0.05
HD 36267	14760	4.27	-0.01
HD 37484	6380	4.54	-0.22
HD 38206	10135	4.36	0.14
HD 38385	6726	3.87	0.02
HD 38393	6163	4.37	0.08
HD 38678	8327	3.97	-0.19
HD 39014	7489	3.41	-0.40
HD 39060	8036	4.21	0.11
HD 40136	7007	4.12	-0.32
HD 41700	6079	4.55	-0.22
HD 41742	6331	4.61	-0.33
HD 43955	17890	4.12	-0.15
HD 66591	16641	4.15	-0.19

Table 3. Continued.

Star	T_{eff} [K]	Log g	[Fe/H]
HD 68456	6305	4.14	-0.39
HD 69830	5586	5.15	0.16
HD 71043	10103	4.31	-0.02
HD 71155	9881	4.22	0.14
HD 75416	12603	4.25	0.16
HD 76151	5750	4.46	-0.16
HD 79108	10273	4.11	-0.07
HD 80950	10330	4.36	-0.05
HD 82943	5764	4.25	0.30
HD 86087	9310	4.25	0.08
HD 88955	8707	4.04	-0.02
HD 98800	4595	3.99	-0.22
HD 99211	10625	4.90	-0.01
HD 102647	8522	4.26	-0.25
HD 105211	6901	3.91	-0.29
HD 105686	9930	4.19	-0.48
HD 108257	16576	3.98	-0.53
HD 108483	20320	4.33	-0.06
HD 109085	6756	4.17	-0.21
HD 109573	9378	4.43	-0.03
HD 111786	8115	3.84	-1.45
HD 113766	6796	4.32	0.09
HD 115617	5558	4.55	0.07
HD 115892	8600	4.11	-0.46
HD 117176	5495	4.02	-0.08
HD 117360	6314	4.51	-0.45
HD 121847	12472	4.00	-0.09
HD 123160	4356	4.10	0.04
HD 124771	16136	4.18	-0.02
HD 128311	4635	4.71	-0.04
HD 131885	9680	4.20	-0.23
HD 135344	6692	4.11	-0.20
HD 136246	9790	4.30	-0.28
HD 139365	17990	4.33	0.17
HD 139664	6693	4.55	-0.31
HD 141569	9963	4.11	-0.07
HD 142096	17034	4.75	-0.27
HD 142114	18429	4.42	0.23
HD 142165	14077	4.31	0.11
HD 144432	6957	3.55	-0.18

Table 3. Continued.

Star	T_{eff} [K]	Log g	[Fe/H]
HD 145482	19214	4.32	-0.24
HD 150638	12453	4.16	-0.42
HD 152391	5418	5.05	-0.12
HD 158643	9772	3.12	-0.25
HD 158793	9781	3.03	0.32
HD 159082	10990	3.91	-0.06
HD 160691	5600	4.30	0.09
HD 161868	8567	3.98	-0.06
HD 164249	6620	4.32	-0.09
HD 164577	9687	3.67	-0.29
HD 165341	5153	4.20	-0.32
HD 166841	10885	3.36	-0.02
HD 169830	6349	4.08	0.08
HD 176638	10095	4.10	-0.21
HD 177817	12667	3.72	0.19
HD 178253	8448	4.01	-0.11
HD 181296	9207	4.30	0.17
HD 181327	6449	4.44	0.29
HD 181869	12100	4.00	0.18
HD 183324	10325	4.17	-1.24
HD 185507	21374	4.59	0.04
HD 188228	10366	4.23	-0.13
HD 191089	6402	4.33	-0.34
HD 198160	7860	4.02	-1.03
HD 199260	6231	4.37	-0.11
HD 203608	6105	4.61	-0.51
HD 206893	6454	4.40	-0.05
HD 207129	5776	4.39	-0.12
HD 209253	6175	4.62	-0.17
HD 216435	5755	3.82	-0.17
HD 216437	5757	3.99	0.20
HD 216956	8743	4.09	-0.34
HD 221853	6196	4.02	0.00
HD 224392	8778	4.06	0.07